NUMERICAL ANALYSIS OF STATE-CHANGING PROCESSES IN GRANULAR ASSEMBLIES

I. Bojtár and K. Bagi

Department of Civil Engineering Mechanics,
Technical University, H-1521, Budapest

Received July 20, 1989

Presented by Prof. dr. S. Kaliszky

Abstract

A discrete model made for the analysis of state-changing processes of granular assemblies is introduced here. Our numerical experiments can help in the analysis of some theoretically suggested variables that could be used later in the macro-level description of the behaviour of granular materials.

1. Introduction

The development in computer technics opened new possibilities in the research of constitutive equations of granular materials. Based on the theoretical results, new kinds of constitutive equations can be derived or previously suggested ideas can be tested.

Thermodynamical constitutive equations are more and more often used. Beside the traditional variables like stress and strain, there are so-called internal variables applied in these equations. In case of granular materials these variables should probably depend on the state of the internal microstructure of the material.

There are several theoretical suggestions how to define internal variables; but most of them have never been tested by numerical or physical experiments. Our aim has been to develop a numerical model able to follow the changes in the microstructure; then to use this model for the analysis of the behaviour of certain suggested variables during state-changing processes. Our final goal is to find state variables that could be efficiently used in the engineering practice.

Our first results will be introduced here.

2. The chosen internal variables

In the early 1980s M. Satake ([1], [2], [3]) suggested an interesting method based on graph theory for the geometrical description of the assemblies. Since his description about the internal state of assemblies seemed to be easy to use and sufficient, we chose these variables to analyse first.

Also in the 1980s, a stress-partitioning method was suggested by P. A. Cundall ([4]); these variables were chosen as the second group of the analysed internal variables.

Before introducing our numerical model, let us briefly summarize these suggestions.

2.1. *The Satake-variables*

Satake modelled the granular material as an assembly of randomly arranged discs in two dimensions, or spheres in three dimensions. We deal with 2D models only.

In a sufficiently large assembly of touching grains the following variables were defined:

— The so-called *fabric tensor*, calculated from the unit normal vectors at contact points, or from the vectors of the *replaced graph* edges (see Figure 1):

$$\varphi_{ij} = \frac{\sum_{p=1}^{N} \left(\sum_{c=1}^{m} \mathbf{n}_i^c \mathbf{n}_j^c \right)}{\sum_{p=1}^{N} \mathbf{m}} = \frac{\sum_{p=1}^{N} \left(\sum_{c=1}^{m} l_i^c l_j^c \right)}{\sum_{p=1}^{N} \sum_{c=1}^{m} l^{c^2}} \quad (i, j = 1, 2). \tag{1}$$

Here N is the number of grains in the analysed domain R; m is the number of contacts of particle p; n_i^c is the unit normal vector at contact c of particle p; $\mathbf{l}_i^c$ is the vector of the graph edge belonging to contact c; l^c is the length of the graph edge (the distance between the centres of the touching grains).

The replaced graph can always be uniquely decided for a given arrangement of discs: the nodes are the centres of the discs, and the edges connect the nodes which correspond to touching grains.

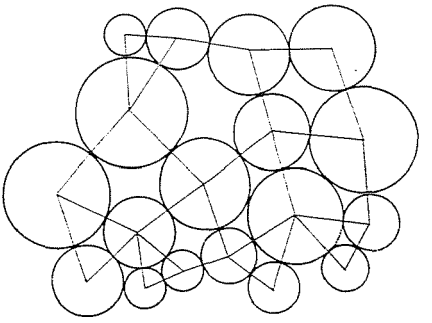

Fig. 1

— The *branch tensor*, a variable that can be considered as a kind of 'weighted fabric tensor' (the weights are the replaced graph edge lengths):

$$\mathbb{B}_{ij} = \frac{\sum_{p=1}^{N} \left(\sum_{c=1}^{m} l^c n_i^c n_j^c \right)}{\sum_{p=1}^{N} \sum_{c=1}^{m} l^c} \tag{2}$$

— The *contact tensor*, also a kind of 'weighted fabric tensor', defined as

$$\mathbb{C}_{ij} = \frac{\sum_{p=1}^{N} \left(\sum_{c=1}^{m} s^c \mathbf{n}_i^c \mathbf{n}_j^c \right)}{\sum_{p=1}^{N} \sum_{c=1}^{m} s^c} \tag{3}$$

where the s^c 'weights' are the lengths of the *dual graph* edges. The dual graph is given by the common tangents of touching grains (see Figure 2).

— The *graph porosity*, based on the two graphs above:

$$v_R = \frac{\bar{A} \sum_{p=1}^{N} \mathbf{m}}{A_R} \tag{4}$$

where $\bar{A}$ is the area defined by the graph edges (see Figure 3), and A_R is the total area of the domain R. $\bar{A}$ can be calculated as

$$\bar{A} = \frac{1}{2} \bar{s} \bar{l} \tag{5}$$

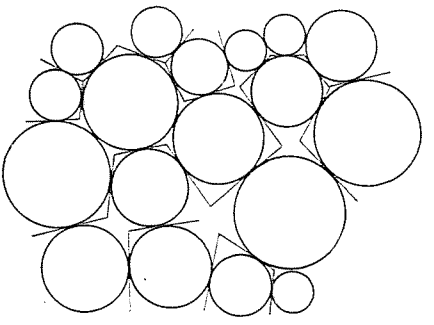

Fig. 2

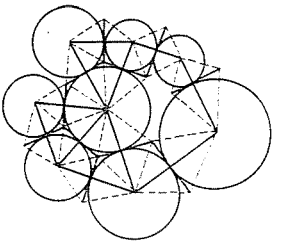

Computation of graph-porosity

Fig. 3

where

$$\bar{l} = \frac{1}{\sum_{p=1}^{N} \mathbf{m}} \sum_{p=1}^{N} \sum_{c=1}^{m} l^c;$$

$$\bar{s} = \frac{1}{\sum_{p=1}^{N} \mathbf{m}} \sum_{p=1}^{N} \sum_{c=1}^{m} s^c;$$

v_R has an interesting physical meaning: the work done by the F contact forces on the corresponding Δu relative displacements can be expressed with the help of the internal work done by the internal stresses on the strains in the following manner:

$$v_R A_R(\sigma_{i,j}\epsilon_{i,j}) = \sum_{(R)} \frac{1}{2} \mathbf{F}\Delta\mathbf{u}. \tag{6}$$

After these geometrical variables, let us see now Cundall's stress partitions.

2.2. Cundall's stress analysis

Similarly to Satake, Cundall modelled the granular material by a $2D$ random assembly of perfectly rigid, touching grains.

From the original domain R an A area can be separated which is not disturbed by any boundary conditions (external loads acting directly on a grain, kinematical constraints, etc.). For the A area the average stress tensor can be defined:

$$\bar{\sigma}_{ij} = \frac{1}{A} \int_{(A)} \sigma_{i,j} dA. \tag{7}$$

If all the grains are circular:

$$\bar{\sigma}_{ij} = \frac{1}{A} \sum_{p=1}^{N} \left(R^p \sum_{c=1}^{m} \mathbf{n}_i^c \mathbf{F}_j^c \right). \tag{8}$$

Here R^p is the radius of particle p, and m is the number of contact points of particle p.

Cundall separated this stress tensor into four partitions:

$$\bar{\sigma}_{ij} = \bar{\sigma}_{ij}(s) + \bar{\sigma}_{ij}(f) + \bar{\sigma}_{ij}(v) + \bar{\sigma}_{ij}(i) \tag{9}$$

where the four partitions are:

$\bar{\sigma}_{ij}(s)$; shear stress tensor
$\bar{\sigma}_{ij}(v)$; normal variation stress tensor
$\bar{\sigma}_{ij}(f)$; fabric stress tensor
$\bar{\sigma}_{ij}(i)$; isotropic stress tensor

First, the total contact force acting at a given contact point of a grain is split into normal and tangential components (see Figure 4). The shear stress is calculated from the tangential forces:

$$\bar{\sigma}_{ij}^s = \frac{1}{A} \sum_{p=1}^{N} R^p \sum_{c=1}^{m} [\mathbf{n}_i^c \mathbf{F}_j^c - (\mathbf{F}_k^c \mathbf{n}_k^c) \mathbf{n}_i^c \mathbf{n}_j^c]. \tag{10}$$

Here $\mathbf{F}_i$ is the total contact force vector as shown in the figure; $\mathbf{n}_i$ is the unit contact normal vector.

This partition corresponds to the mobilized shear forces; it is related to the tendency of the contacts to slide, so related to the dissipation of energy during the state-changing process.

In the second step the average normal force belonging to the grain is separated from each normal force acting on the grain. From the remaining part, the normal variation stress component is calculated:

$$\bar{\sigma}_{ij}^v = \frac{1}{A} \sum_{p=1}^{N} R^p \sum_{c=1}^{m} \left[(\mathbf{F}_k^c \mathbf{n}_k^c) \mathbf{n}_i^c \mathbf{n}_j^c - \left[\frac{1}{m} \sum_{c=1}^{m} (\mathbf{F}_k^c \mathbf{n}_k^c) \right] \mathbf{n}_i^c \mathbf{n}_j^c \right]. \tag{11}$$

This partition corresponds to the variation in the magnitude of normal forces with angle; it reflects the eccentricity of forces acting on the grains, similarly to the classical buckling problems.

The remaining part of the stress tensor may be split into the isotropic component

$$\bar{\sigma}_{ij}(i) = \delta_{ij} \bar{\sigma}_0 = \frac{\delta_{ij}}{A(\delta_{kk})} \sum_{p=1}^{N} R^p \sum_{c=1}^{m} (\mathbf{F}_k^c \mathbf{n}_k^c) \tag{12}$$

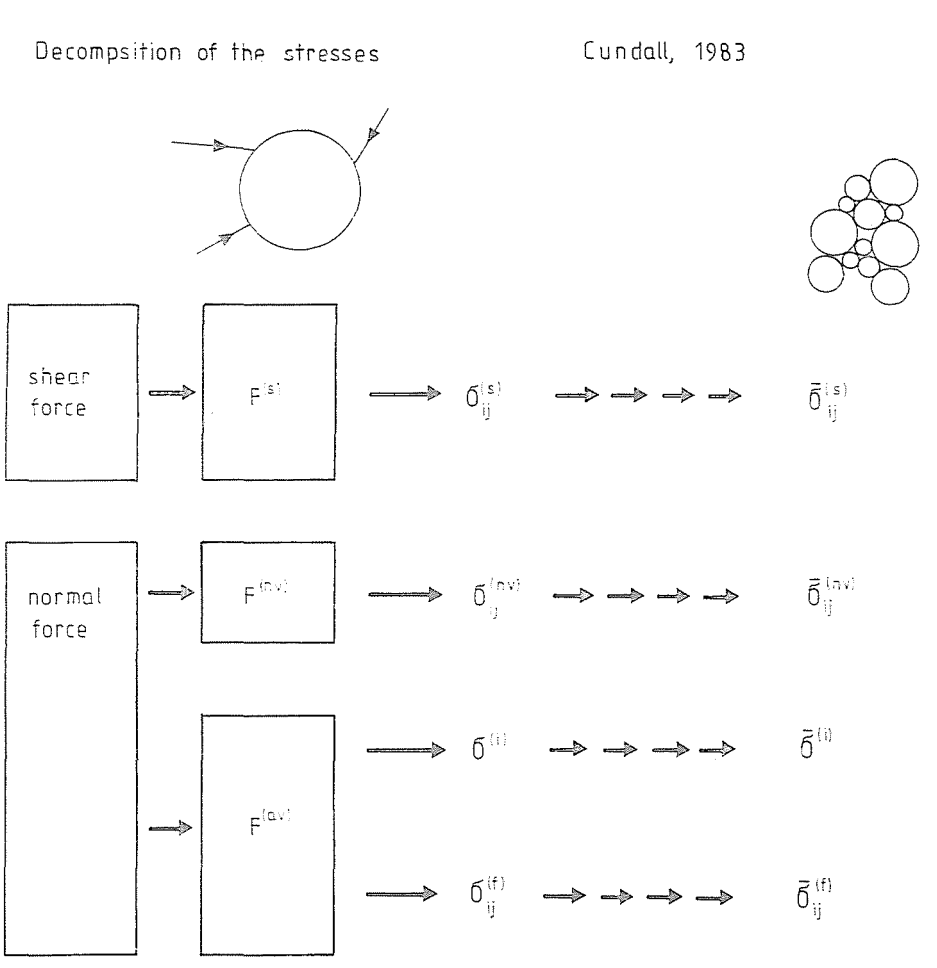

Fig. 4

and into the fabric partition

$$\sigma_{ij}^{f} = \left[\frac{1}{A}\sum_{p=1}^{N} R^{p} \sum_{c=1}^{m} \mathbf{F}^{p(av)}\, \mathbf{n}_i^c \mathbf{n}_j^c\right] - \sigma_0 \delta_{ij} \tag{13}$$

that corresponds to the angular distribution on contact points thereby related to the anisotropy of the microstructure.

We intend to analyse how these stress partitions change during loading processes, how they are influenced by the rearrangement of the microstructure, etc.

And now let us introduce the numerical model.

3. Numerical model for the analysis of state-changing processes

The calculations are based on the classical displacement method. The unknowns are the horizontal and the vertical displacements and the rotations of the grains (see Figure 5):

$$\mathbf{u}^{(i)} = \begin{bmatrix} u_x^{(i)} \\ u_y^{(i)} \\ \omega^{(i)} \end{bmatrix}. \tag{14}$$

The external loads consist of the following three components corresponding to the displacements:

$$\mathbf{f}^{(i)} = \begin{bmatrix} f_x^{(i)} \\ f_y^{(i)} \\ f_M^{(i)} \end{bmatrix}. \tag{15}$$

The relation between the relative displacements and the contact forces acting at the contact point of two grains is described by the 'micro-material-law' of the contact. At present two types of contacts are used in the model. In the first case (materials like concrete) the contact is rigid; beside the normal and shear forces, bending moment is also possible (see Figure 6/a). In the second case (materials like sand) the contact resists compression and shear force only.

Relative displacements can be calculated from the absolute displacements of the grains by transformation matrices:

$$\mathbf{v}^c = \mathbb{T}^{c(j)}\mathbf{u}^{(j)} - \mathbb{T}^{c(i)}\mathbf{u}^{(i)} \tag{17}$$

where the $\mathbb{T}$ matrices are:

$$\mathbb{T}^{c(j)} = \begin{bmatrix} \cos\alpha^c & \sin\alpha^c & 0 \\ -\sin\alpha^c & \cos\alpha^c & R^{(j)} \\ 0 & 0 & 1 \end{bmatrix}$$
$$\mathbb{T}^{c(i)} = \begin{bmatrix} \cos\alpha^c & \sin\alpha^c & 0 \\ -\sin\alpha^c & \cos\alpha^c & -R^{(i)} \\ 0 & 0 & 1 \end{bmatrix}. \tag{18}$$

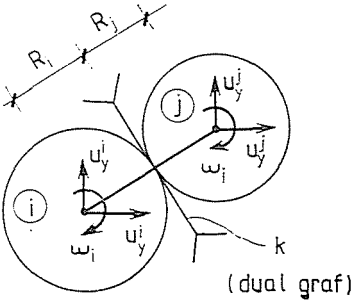

Fig. 5

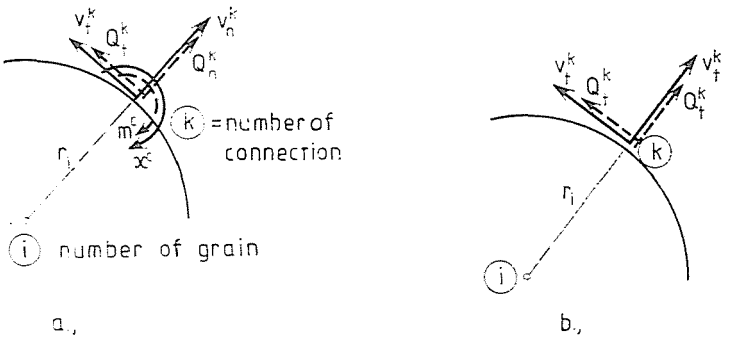

Fig. 6

The external loads and the contact forces acting on a given grain have to be in equilibrium:

$$\mathbf{f}^{(i)} = \sum_{c=1}^{m} \mathbf{T}^{c(i)^T} \mathbf{Q}^c. \tag{19}$$

The 'micro-material-law' of the contact is expressed by the contact stiffness matrix $\mathbf{k}^c$:

$$\mathbf{Q}^c = \mathbf{k}^c \mathbf{v}^c. \tag{20}$$

In total lack of experimental data we have only assumptions about $\mathbf{k}^c$. The contact stiffness matrix assumed for the first type of contacts is:

$$\mathbf{k}^c = \begin{bmatrix} Es & 0 & 0 \\ 0 & Gs & 0 \\ 0 & 0 & \dfrac{Es^3}{12} \end{bmatrix} \tag{21}$$

where the shear stiffness depends on the normal stress acting at the contact:

$$G = G_0 - \frac{\mu v_n E}{s}.$$

Here E is the normal elastic modulus, G_0 is the initial shear modulus, s is the length of the dual graph edge which belongs to the contact, and μ is a 'frictional' factor.

Figure 7 shows the relation between each relative displacement and the corresponding contact force. If one of the contact force components exceeds a limit value, the contact is broken.

In the second case $\mathbf{k}^c$ has a simpler form:

$$\mathbf{k}^c = \begin{bmatrix} Es & 0 & 0 \\ 0 & \bar{G}s & 0 \\ 0 & 0 & 0 \end{bmatrix} \tag{22}$$

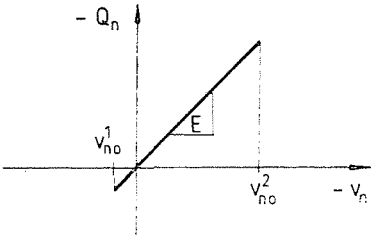

Connection between the normal force and the relativ displacement

a.,

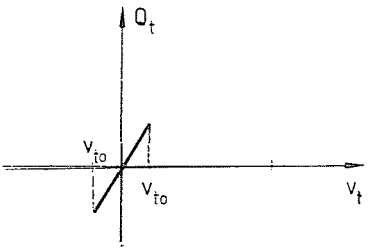

Shear force-relativ displacement

b.,

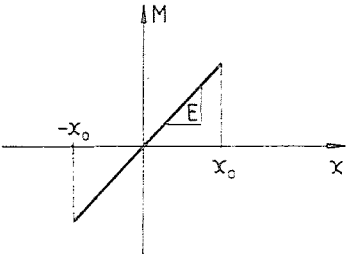

Bending moment and relativ displacement

c.,

Fig. 7

where

$$\bar{G} = \bar{G}_0 - \frac{\mu v_n E}{s}$$

$\bar{G}_0$ can be assumed to be much smaller than G_0.

Inserting (17) into (20), and using it to express (19), we get the equilibrium equations of a given grain:

$$\mathbf{f}^{(i)} = \sum_{c=1}^{m} \mathbb{T}^{c(i)^T} \mathbb{k}^c \mathbf{v}^c. \tag{23}$$

These equations can be collected for all grains so the global equilibrium of the assembly are given:

$$\mathbf{F} = \mathbb{K}_{\text{glob}} \mathbf{u}. \tag{24}$$

(24) gives the relationship between the absolute displacements of the grains and the external forces, similarly to the classical finite element solutions.

The behaviour of the assembly is basically determined by the parameters used in (21) and (22).

(24) is a physically non-linear problem: as it can be seen in Figure 7:

$$\mathbb{K}_{\text{glob}} = \mathbb{K}_{\text{glob}}(\mathbf{Q}_n, \mathbf{Q}_t(v_n), \mathbf{Q}_M). \tag{25}$$

4. The analysis

The analysed assembly (Figure 8) is bounded by a rectangular area. The sizes of this area have to be given first; the randomly generated grains are dropped down into this 'box', one after the other.

Every grain must find a stable position by being supported by the others or by the edges of the area so that this procedure would lead to a stable structure.

The radius of the grains randomly changes between a given minimum and maximum value; any given sieve curve can be simulated.

Different contact properties can be prescribed in given horizontal and vertical strips of the area, or the different contact types can be randomly distributed in the assembly.

Any grain can be fixed or have prescribed displacements. In our recent model the loads consist of concentrated forces or moments acting directly on the grains, or linearly distributed forces acting on the edges of the area.

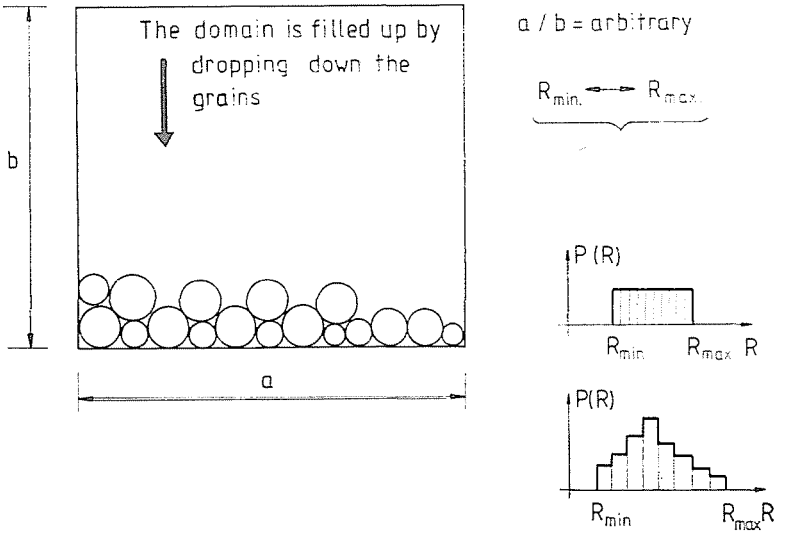

Fig. 8

We apply the widely used Newton-Raphson method to follow the state-changing process. The loading process is given by a series of load steps. In a given load step the change of the stiffnesses is followed by iteration steps until the equilibrium state that belongs to the load step is found; the analysed variables can be calculated in the equilibrium states or in all iteration steps.

5. Numerical examples

Two simple examples will be introduced to illustrate the usability of the model. Experiments on really characteristic assemblies containing 800—1000 grains have just been started.

Figure 9 shows an example consisting of three discs with uniform radius. The horizontal displacement of grain 2. is shown in Figure 10/a. As it can be seen in Figure 10/b, the behaviour of the model is very similar to the Doughil-models used in continuum-mechanics for the description of elastic-fracturing materials.

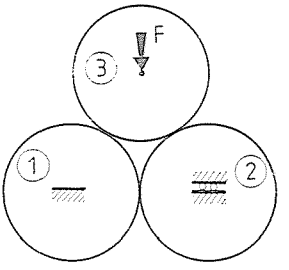

Fig. 9

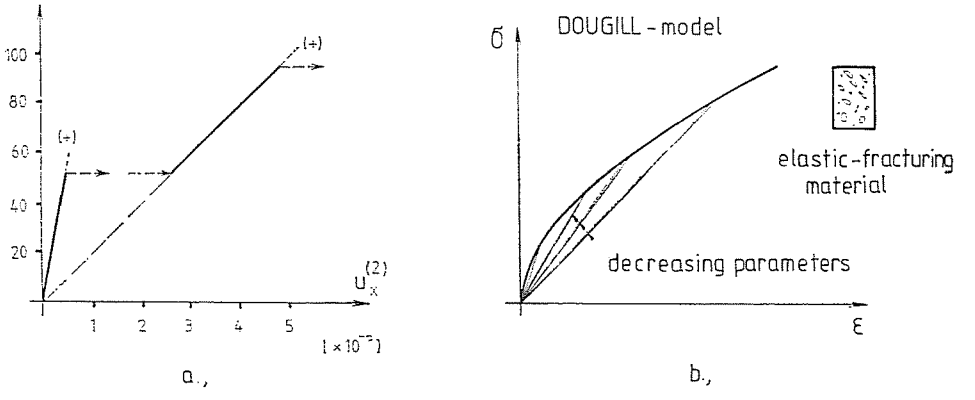

Fig. 10

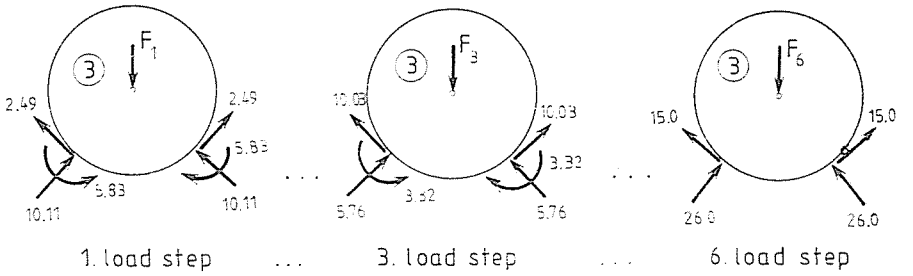

Fig. 11

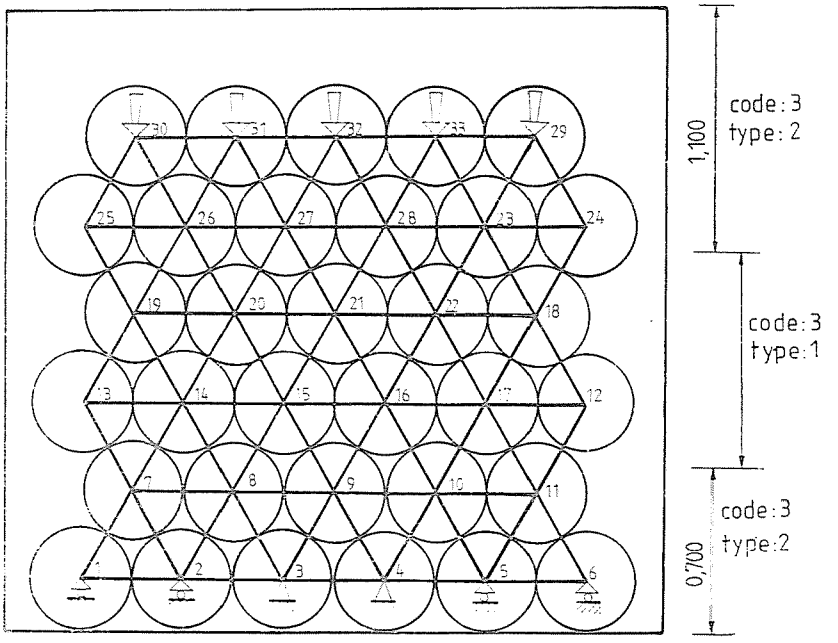

Fig. 12

Figure 11 shows the forces acting on grain 3. in different load steps.

An assembly that consists of 32 grains can be seen in Figure 12. The assembly is loaded by uniform compression. Stronger contacts are applied in two strips of the area to avoid local fracture around the concentrated forces and the supports.

Figure 13 shows the change of the replaced graph during the state-changing process. Each graph edge corresponds to a contact so the crashing of the assembly can be followed this way.

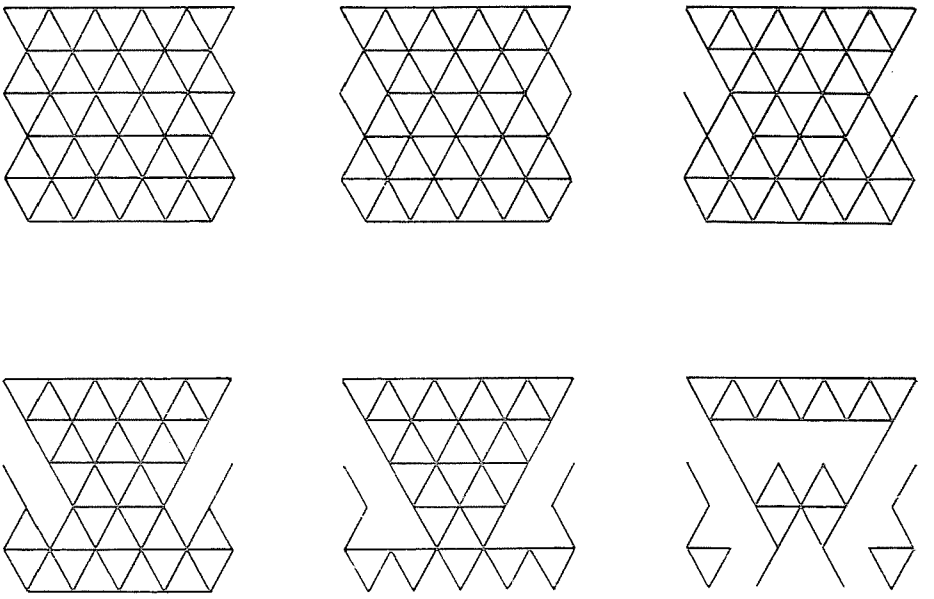

Fig. 13

The Cundall-partitions are calculated during the process:

Loadstep; Loadfactor	$\bar{\sigma}_{ij(s)}$	$\bar{\sigma}_{ij(v)}$	$\bar{\sigma}_{ij(f)}$	$\bar{\sigma}_{(i)}$
1. (1.00)	$\begin{bmatrix} 5.305 & 0 \\ 0 & -5.305 \end{bmatrix}$	$\begin{bmatrix} 8.843 & 0 \\ 0 & -8.843 \end{bmatrix}$	$\begin{bmatrix} .744 & 0 \\ 0 & -.744 \end{bmatrix}$	−15.180
2. (1.20)	$\begin{bmatrix} 6.459 & 0 \\ 0 & -6.459 \end{bmatrix}$	$\begin{bmatrix} 10.530 & 0 \\ 0 & -10.530 \end{bmatrix}$	$\begin{bmatrix} .892 & 0 \\ 0 & -.893 \end{bmatrix}$	−18.206
3. (1.40)	$\begin{bmatrix} 7.628 & 0 \\ 0 & -7.628 \end{bmatrix}$	$\begin{bmatrix} 12.203 & 0 \\ 0 & -12.203 \end{bmatrix}$	$\begin{bmatrix} 1.039 & 0 \\ 0 & -1.039 \end{bmatrix}$	−21.231
4. (1.60)	$\begin{bmatrix} 8.811 & 0 \\ 0 & -8.811 \end{bmatrix}$	$\begin{bmatrix} 13.865 & 0 \\ 0 & -13.865 \end{bmatrix}$	$\begin{bmatrix} 1.186 & 0 \\ 0 & -1.186 \end{bmatrix}$	−24.255
5. (1.80)	$\begin{bmatrix} 10.363 & 0 \\ 0 & -10.363 \end{bmatrix}$	$\begin{bmatrix} 13.651 & 0 \\ 0 & -13.651 \end{bmatrix}$	$\begin{bmatrix} 2.784 & 0 \\ 0 & -2.784 \end{bmatrix}$	−27.333

In this case the dominant part is the isotropic compression component; the shear and normal ariation partitions are also significant. The fabric stress partition that measures the anisotropy is negligible now.

6. Further development

At present we are working on the analysis of the behaviour of the Stake- and Cundall-parameters in large assemblies loaded until crashing.

We intend to determine the parameters used in the micro-material-laws by identification examinations. The behaviour of the model could be compared with the results of simple physical experiments (shearing tests, linear tension etc.)

Numerically and theoretically it will be one of the most complicated problems how to take into consideration the effects of large displacements of the grains; the solution of this problem is indispensable for the proper analysis of sand-like assemblies.

References

1. SATAKE, M.: Fundamental Quantities in the Graph Approach of Granular Materials (US-Japan Seminar on the 'New Models and Constitutive Relations in the Mechanics of Granular Materials', Aug. 23—27. 1982. Cornell University, USA).
2. SATAKE, M.: On Fabric Tensor in Granular Materials. (Mechanical Const. Equations of Granular Materials., ed. by M. Satake, 1982. Tokyo).
3. KISHINO, Y.—SATAKE, M.: A New Simulation Method for Granular Materials (Acta Stereol. 1987; 6/III: 365—371. Proc. ICS VII. Caen 1987).
4. CUNDALL. P. A.—STRACK, O. D. L.: Modelling of Microscopic Mechanisms in Granular Material (Mechanics of Granular Materials: New Models and Const. Relations, ed. J. T. Jenkins and Satake, Elsevier publ., 1983. Amsterdam).

Dr. Imre BOJTÁR
Katalin BAGI
H-1521, Budapest